IDENTIFICATION OF APIGENIN AND LUTEOLIN ISOLATED FROM THE AERIAL PARTS OF *BACOPA MONNIERI* (L.) WETTST *IN VITRO* EVALUATION OF *α*-AMYLASE AND *α*-GLUCOSIDASE INHIBITION ACTIVITY

Aye Aye Thant[1], Yi Yi Win[2], Myint Myint Khine[3], Ni Ni Than[4]

Abstract

The present research deals with the analysis to isolate organic compounds and examine antidiabetic activity from the aerial parts of the Bacopa monnieri (Byone-hmwe) plant collected from the Twantay Township, Yangon Region. By column and thin layer chromatography, apigenin (AAT-2) and luteolin (AAT-3) were isolated from the active ethyl acetate fraction and identified by using UV, FT IR, 1HNMR, and NMR spectroscopic methods. The spectrophotometric method was used to determine the antidiabetic activity of a drug using metformin, an oral hypoglycemic agent, as a positive control for the inhibition effect on α-amylase and α-glucosidase enzymes. The α-amylase inhibitory effect (IC_{50}= 54.09 μg/mL,78.14 μg/mL) and *α*-glucosidase inhibitory effect (IC_{50} = 62 μg/mL, 91.66 μg/mL) were observed in ethanol and watery extracts. Furthermore, apigenin and luteolin inhibited α-amylase (IC_{50}= 1.049 μg/mL, 0.75 μg/mL) and α-glucosidase (IC_{50} = 0.558 μg/mL, 0.507 μg/mL), which was comparable with the standard drug metformin (IC_{50} = 0.497 μg/mL). The percentage of enzyme inhibition of isolated luteolin was nearly the same as that of standard metformin.

Keywords: *Bacopa monnieri*, *α*-amylase inhibition, *α*-glucosidase inhibition, apigenin, luteolin

Introduction

Bacopa monnieri, an important medicinal plant of the family Scrophulariaceae is used in the traditional medicine to treat various nervous disorders and to promote memory and intellect. Some important medicinal uses of the plant *B. monnieri* are the treatment of different diseases and its traditional formulation (Lal and Baraik, 2019). Flavonoids are a major group of polyphenolic compounds that have been reported to possess inhibitory activity against α-glucosidase (Williams, 2013). In relation to their structure, the number and position of their hydroxyl groups in the molecule are determining factors for enzyme inhibition. The inhibitory activity increased considerably with an increase in the number of hydroxyl groups on the B ring. Animal experiments revealed that ethanol extracts of *B. monnieri* have a positive effect on haemoglobin glycosylation *in vivo*, anti-oxidant potential, and *in vitro* peripheral glucose utilization. Bacoside, a triterpenoid isolated from the plant extract, has been found to increase glycogen content in the liver of diabetic rats and peripheral glucose utilization in the diaphragm (Ghosh *et al*., 2011). The current study aims to isolate and identify the two flavones, apigenin (AAT-2) and luteolin (AAT-3), from *B. monnieri's* aerial parts and to determine their antidiabetic activity.

Botanical Aspect of *Bacopa monnieri* (L.) Wettst (Byone-hmwe)

Family: Plantaginaceae
Botanical name: *Bacopa monnieri* (L.) Wettst.
Myanmar name: Byone-hmwe
Part used: the aerial parts

Figure 1. *Bacopa monnieri*

[1] Department of Chemistry, University of Yangon,
[2] Department of Chemistry, Hpan-an University
[3] Myingyan University
[4] Department of Chemistry, University of Yangon

Materials and Methods

Plant Material

The sample was collected from Twantay Township, Yangon Region, in July 2019 and identified as *Bacopa monnieri* (L) Wettest, by the authorized botanist at the Department of Botany, University of Yangon. The sample was dried under the shade for a week, cut into very small pieces, and then ground into a purely fine powder using an electric grinder. The powdered sample was stored in airtight containers.

Extraction and Isolation of Pure Compounds (AAT-2 and AAT-3)

Dried powder (1000 g) of aerial parts of *B. monnieri* was extracted with 95% ethanol. After evaporation of the solvent, the resulting crude extract was successively partitioned between organic solvents (petroleum ether, ethyl acetate) and water. The ethyl acetate crude extract (11 g) was chromatographically separated on silica gel 60 (70-230 mesh, Merck) with a petroleum ether and ethyl acetate mixture used as an eluent, varying solvent ratios from non-polar to polar. Each and every fraction was checked with TLC and a UV detector. The fractions with the same R_f values were combined, and six combined fractions were obtained. Among them, the combined fraction (V) was rechromatographed by using the same adsorbent and eluent as mentioned in the previous column. Pure pale-yellow and yellow crystals were obtained and checked on TLC for purity. It gave one spot on TLC (R_f = 0.5) and (R_f = 0.4) with pet-ether: ethyl acetate (1:1) (v/v). The weight of the isolated compounds (AAT-2) was 50 mg and (AAT-3) was 30 mg, and their yield percents were found to be 1.25% and 0.75% based on the ethyl acetate crude extract, respectively. The FT IR and UV-vis spectra were measured at the Department of Chemistry, University of Yangon and ^{1}H NMR and ^{13}C NMR were measured at the Division of Natural Product Chemistry, Institute of Natural Medicine, and University of Toyama, Japan.

Screening of *In vitro* Antidiabetic Activity

In diabetes, the body cannot produce enough insulin or uses insulin, and it is diagnosed by observing raised levels of glucose in the blood (Khadayat et al., 2020). One of the therapeutic approaches to controlling postprandial hyperglycemia in T2DM is to inhibit the digestion of dietary carbohydrates. Pancreatic α-amylase (E.C.3.2.1.1) is a key enzyme that breaks down dietary carbohydrates such as starch into simple monosaccharides in the digestive system. These are further degraded by α-glucosidases to glucose, which, on absorption, enters the bloodstream. Therefore, inhibiting the α-amylase and α-glucosidase enzymes, for example, can suppress carbohydrate digestion, delay glucose uptake, and, as a result, lower blood sugar levels.

Determination of *α*-Amylase Inhibition Activity

The α-amylase enzyme inhibition potential was assessed using a 3, 5-dinitrosalicylic acid (DNSA) assay (Kajaria *et al*., 2013). The reaction mixture contained 1mL of phosphate buffer (0.04 M, pH = 6.9), 1 mL of α–amylase: 1 U/mL, and 1 mL of varying concentrations of ethanol and watery extracts. Apigenin (AAT-2) and luteolin (AAT-3) were preincubated at 37 ℃ for 20 min. Next, 0.4 mL of 1% soluble starch (0.004 M phosphate buffer pH 6.9) was added as a substrate and incubated at 37℃ for 30 min; 0.6 mL of the 3, 5-dinitrosalicylic acid (DNS) reagent was then added and boiled for 20 min. The absorbance of the resulting mixture was assessed at 540 nm using a UV spectrophotometer. Metformin, a well-known α-amylase inhibitor, is an excellence standard in a wide range of concentrations. Samples without plant extracts were used controls, as the blank solution (without amylase) and each test was carried out in triplicate. The outcome was expressed as percentage inhibition, which was calculated using the following equation.

$$\% \text{ Inhibition} = \frac{C-(A-B)}{C} \times 100$$

Where A= absorbance of the sample

B = absorbance of blank (without amylase)

C = absorbance of the control (without test sample)

Standard deviation (SD) and 50% inhibition concentration (IC_{50}) values were calculated by the linear regression programme.

Determination of *In vitro α*-Glucosidase Inhibitory Assay

The effect of the plant extracts on *α*-glucosidase activity was determined according to the method described by Kim *et al*., 2011. The substrate solution, *p*-nitrophenyl glucopyranoside (PNPG), was prepared in 0.04 M phosphate buffer, at pH 6.9. 1 mL of *α*-glucosidase (0.5 U/mL) was preincubated at 37 ℃ for 20 min with 1 mL of the ethanol and water extracts and isolated compounds; apigenin (AAT-2) and luteolin (AAT-3). Then 0.5 mL of 0.003 M (PNPG) as a substrate dissolved in 0.04M phosphate buffer (pH 6.9) was added to start the reaction. The reaction mixture was then incubated at 37 ºC for 20 min and stopped by adding 1 mL of 0.1 M Na_2CO_3. The *α*-glucosidase activity was determined by measuring the yellow-coloured *p*-nitrophenol released from PNPG at 405 nm using a UV spectrophotometer. Samples without plant extracts were used as controls and as the blank solutions (without amylase) and each test was carried out in triplicate. The outcome was expressed as percentage inhibition, which was calculated using the following equation.

$$\% \text{ Inhibition} = \frac{C-(A-B)}{C} \quad 100$$

Where, A = absorbance of the sample

B = absorbance of blank (without amylase)

C = absorbance of the control (without test sample)

Standard deviation (SD) and 50% inhibition concentration (IC_{50}) values were calculated by the linear regression programme.

Results and Discussion

The *α*-amylase is found in saliva and pancreatic juice, which hydrolyzes alpha-linked polysaccharides' alpha bonds like in starch and glycogen, resulting in glucose and maltose that can quickly enter the bloodstream. It is the primary amylase type present in humans and other mammals. Inhibition of *α*-amylase delays the digestion process by hampering the breakdown of starch in the intestine and, hence, can be utilized as an effective strategy for regulating hyperglycemic conditions (Oyedemi *et al.*, 2017). The plant extract showed potent inhibition of α-amylase activity. The active components in the extract compete with the substrate for binding to the active site of the enzyme, preventing the breakdown of the oligosaccharide to disaccharides. This demonstrates that the inhibition percentage increases with the concentration of the extract increased. The highest percent of α-amylase inhibition and the lowest IC_{50} value inhibitors of α-glucosidase delay the breakdown of carbohydrates in the small intestine and diminish the postprandial blood glucose excursion in a person suffering from diabetes (Ogunwande *et al*., 2007). The plant extract exhibited potent inhibition of α-glucosidase activity such that the active components in the extract do not compete with the substrate for binding to a separate site on the enzyme to retard the conversion of disaccharides to monosaccharides (Mogale *et al*., 2011).

The present finding reveals that *B. monnieri'*s aerial parts efficiently inhibit the *α*-amylase and α-glucosidase enzymes. The enzyme inhibition activity of ethanol and watery extracts, and isolated compounds; apigenin (AAT-2), and luteolin (AAT-3) was evaluated by a UV spectroscopic method. From the mean absorbance values, the α-amylase and α-glucosidase inhibition of ethanol extract (IC_{50} = 54.09 µg/mL) and (IC_{50} = 62.5µg/mL) had more inhibitory potential than watery extract (IC_{50} = 78.14 µg/mL) and (IC_{50} = 91.66 µg/mL) as shown in Tables 1, and 2, and Figures 2 and 3. In contrast, the isolated compound, luteolin (IC_{50} = 0.558 µg/mL) more effectively inhibited enzyme activity than apigenin (IC_{50}=1.049 µg/mL), respectively (Table 3, Figure 4). In these assay methods, metformin was used as the positive control. In comparison to metformin, luteolin had the highest anti-diabetic activity, followed by ethanol and watery extracts, as well as apigenin (Table 4, Figure 5).

Table 1. IC_{50} Values of *α*-Amylase Inhibitory Activity of Crude Extracts of the Aerial Parts of *B. monnieri*

Samples	**% Inhibition in Different Concentrations (µg/mL)**						**IC_{50} (µg/mL)**
	31.25	**62.5**	**125**	**250**	**500**	**1000**	
Ethanol extract	33.89 ± 0.01	55.93 ± 0.57	62.71 ± 0.42	71.18 ± 0.33	88.13 ± 1.12	94.91 ± 0.98	54.09
Watery extract	27.11± 1.10	44.89 ± 0.02	65.30 ± 0.56	77.55 ± 0.66	83.69 ± 1.40	95.91 ± 0.46	78.14
*Standard metformin	46.93 ± 0.26	63.26 ± 0.02	77.55 ± 0.03	79.59 ± 0.37	85.71 ± 0.48	96.37 ± 1.98	45.31

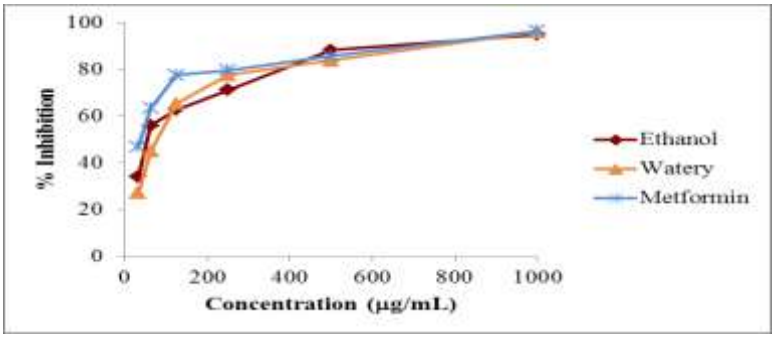

Figure 2. A plot of α-amylase inhibition activity versus concentrations of crude extracts of the aerial parts of *B. monnieri*

Table 2. IC_{50} Values of α-Glucosidase Inhibitory Activity of Crude Extracts of the Aerial Parts of *B. monnieri*

Sample	% Inhibition in Different Concentrations (µg/mL)						IC_{50} (µg/mL)
	31.25	62.5	125	250	500	1000	
Ethanol extract	36.20 ± 1.03	50.00± 0.92	67.24 ± 0.48	75.86 ± 1.11	82.75 ± 1.40	94.82 ± 0.40	62.50
Watery extract	29.31± 0.48	37.93 ± 0.90	63.79 ± 0.25	70.68 ± 1.50	79.31 ± 0.87	89.65 ± 1.21	91.66
*Standard metformin	41..37 ± 0.08	55.17 ± 0.73	62.06 ± 0.21	77.41± 1.07	86.2 ± 1.33	93.1 ± 0.40	50.79

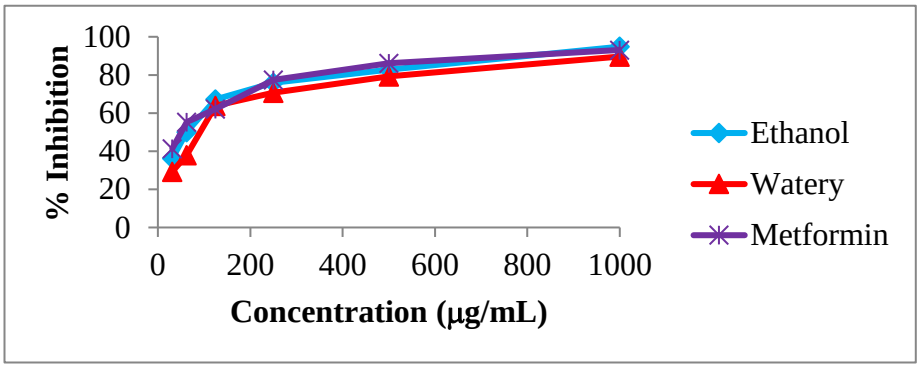

Figure 3. A plot of α-glucosidase inhibition activity versus concentrations of crude extracts of the aerial parts of *B. monnieri*

Table 3. IC_{50} Values of α- Amylase Inhibitory Activity of Isolated Compounds AAT-2 and AAT-3 of the Aerial Parts of *B. monnieri*

Samples	% Inhibition in Different Concentrations (µg/mL)						IC_{50} (µg/mL)
	0.3125	0.625	1.25	2.5	5	10	
AAT-2	24.56± 0.11	36.84± 0.28	52.63± 0.56	63.15± 0.93	80.70± 0.21	92.98± 2.73	1.049
AAT-3	40.35± 0.69	52.67± 0.56	63.15± 0.48	78.94± 0.32	89.47± 0.15	94.73± 1.73	0.558
*Standard metformin	36.59± 1.53	57.89± 0.31	64.91± 0.48	77.19± 0.81	85.96± 0.82	96.49± 0.73	0.497

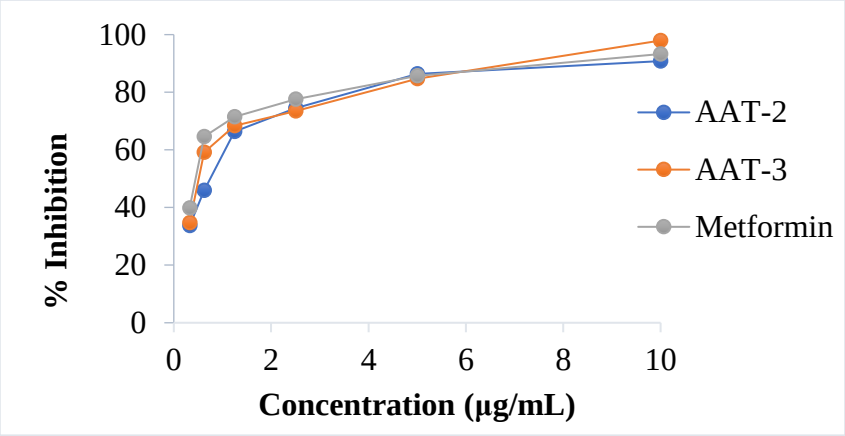

Figure 4. A plot of α-amylase inhibition activity versus concentrations of crude extracts of the aerial parts of *B. monnieri*

Table 4. IC_{50} Values of α-glucosidase Inhibitory Activity of Isolated compounds AAT-2 and AAT-3 of the Aerial Parts of *B. monnieri*

Sample	% Inhibition in Different Concentrations (µg/mL)						IC_{50} (µg/mL)
	0.3125	0.625	1.25	2.5	5	10	
AAT-2	33.67± 1.03	45.91± 0.48	66.32± 0.90	74.48± 0.87	86.33± 1.07	90.81± 1.33	0.750
AAT-3	34.69± 0.92	59.18± 1.01	68.36± 0.87	73.46± 0.48	84.69± 1.41	97.95± 1.11	0.508
*Standard metformin	39.82± 1.21	64.60± 0.73	71.42± 1.02	77.55± 1.41	85.71± 0.25	93.27± 1.50	0.441

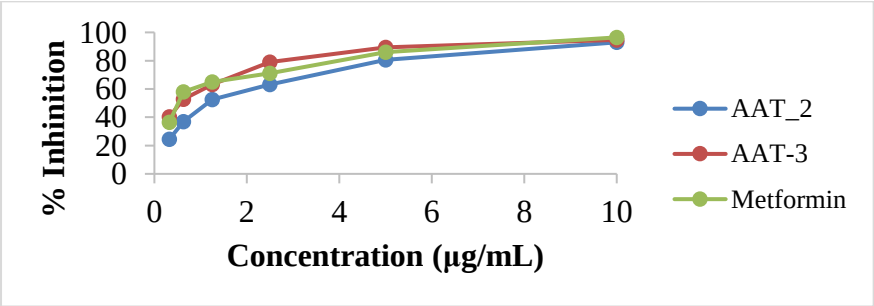

Figure 5. A plot of α-glucosidase inhibition activity versus concentrations of isolated compounds of the aerial parts of *B. monnieri*

Structure Elucidation of Antidiabetic Active Isolated Compound (AAT-2)

The compound AAT-2 was isolated from an ethyl acetate extract of *B. monnieri*. It was obtained as pale-yellow crystals by using PE: EA = 1:1; the R_f value is 0.5. It may be a flavonoid compound because it gave off a red colour when treated with Mg/HCl and a brown colour when reacted with 10% $FeCl_3$.The UV-vis spectra of AAT-2 showed the flavonoid bands II and I in methanol at 268 nm and 336 nm respectively. This absorption band is in agreement with a flavone (band II, 210-280 and band I, 310-350 nm). The UV spectrum in NaOH exhibited a 57 nm

bathochromic shift of the main absorption (band I) with increasing intensity. That indicated the presence of free 4' and 7 hydroxy groups. A 7 nm bathochromic shift of band II in the presence of NaOAc in MeOH also indicated that AAT-2 possessed a 7 hydroxy group and the UV-vis spectrum in $AlCl_3$/HCl produced a 45 nm bathochromic shift of band I, suggesting the presence of 5 hydroxy group. No hypochromic shift was observed in band I of the $AlCl_3$ spectrum, indicating the absence of *ortho*-dihydroxy groups. The UV-vis spectral properties in various shift reagents of AAT-2 were found to be identical to those of the 5, 7, and 4′trihydroxy flavone (Ei Shoubaky *et al.*, 2016).

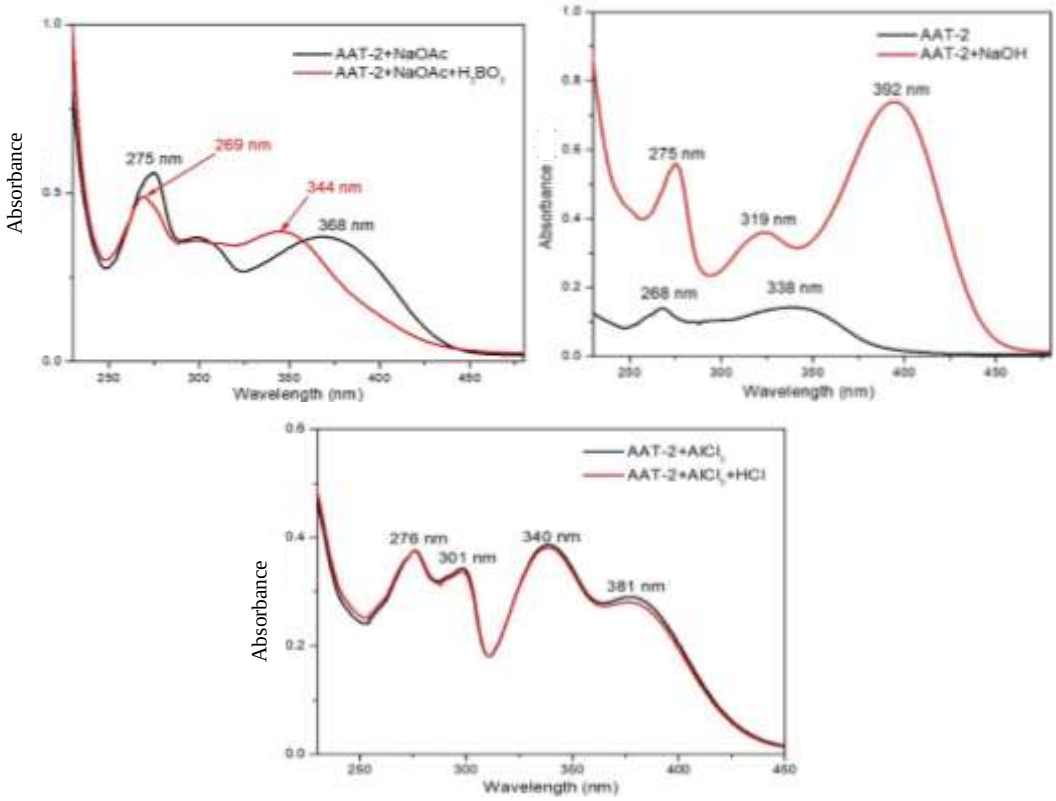

Figure 6. UV spectra of an isolated compound Apigenin (AAT-2) by using shift reagents

In the FT IR spectrum of compound AAT-2, the strong and broad absorption band that appeared at 3274 cm^{-1} indicated the presence of a hydroxyl group. The strong band at 1650 cm^{-1} was due to the C=O stretching vibration of a carbonyl group. The C=C stretching vibration showed at 1604, 1555, and 1495 cm^{-1}. Moreover, asymmetric and symmetric stretching vibration (C-O-C) was described at 1267 cm^{-1} (Figure 7).

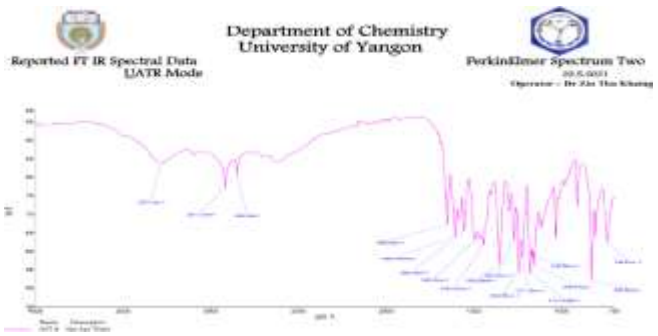

Apigenin (pale yellow crystals)

10% $FeCl_3$

Figure 7. FT IR spectrum of an isolated compound apigenin (AAT-2)

The ^{1}H NMR spectrum of compound AAT-2 (Figure 8) contained 15 protons. The ^{1}H NMR was taken in the deuterated dimethyl sulphoxide, and the proton at positions 2' and 6' due to symmetry appeared as a doublet at 7.091 ppm, and the proton at positions 3' and 5' at 6.091 ppm, upfield due to the neighbouring electron-donating hydroxyl group. The single olefinic proton of the H-3 singlet and two meta-coupled aromatic protons at H-8 and H-6 gave doublet signals at 5.64 and 5.35 ppm. The ^{13}C NMR spectrum indicated the presence of 15 signals, including one carbonyl group, and seven quaternary carbon signals. The ^{13}C NMR spectrum is shown in Figure 8. The carbon signals were observed for seven methine signals at δc 103.2 (C-3), 99.2 (C-6), 94.3 (C-8), 128.8 (C-2' & 6'), 116.3 (C-3' & 5'), and seven quaternary carbon signals at δc 164.1 (C-2), 161.5 (C-5), 164.5 (C-7), 157.7 (C-9), 104.0 (C-10), 121.5 (C-1'), 161.8 (C-4'). One carbonyl signal was also observed at 182.1 (C-4). From the basis of the observed melting point, some physicochemical tests, and all spectral data compared with reported data of apigenin (Kalpana and Rajasekaran 2018), the isolated compound AAT-2 was identified as apigenin ($C_{15}H_{10}O_5$).

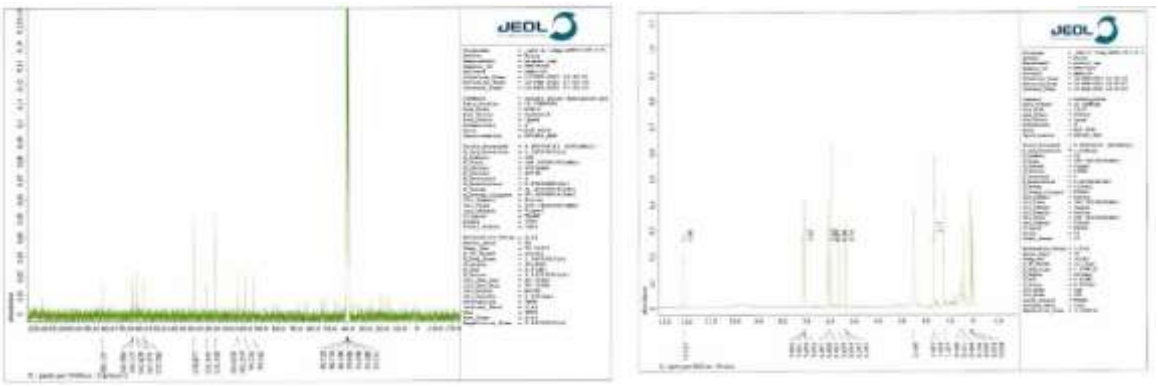

Figure 8. ^{1}H NMR (DMSO-d_6, 400 MHz) and ^{13}C NMR (DMSO-d_6, 100 MHz) spectra of apigenin AAT-2

Compound **AAT-2** (Apigenin): A pale yellow crystal crystallized from pet-ether/EtOAc, (1:1) mp: 345 ℃.; FT IR (ν, cm^{-1}): 3274 (ν_{O-H}), 1650 ($\nu_{C=O}$), 1604,1555,1495 ($\nu_{C=C}$), 1267 (ν_{C-O-C}), 1015 (δoop(C-H)), UV$_{max}$ (MeOH) nm: 268, 338; NaOAc nm: 275,368; NaOAc + H_3BO_3 nm: 269, 344; $AlCl_3$ nm: 276, 340, 381; $AlCl_3$ + HCl nm: 276, 381; NaOH nm: 275,393.^{1}H NMR (400 MHz, DMSO-d_6) δ_H (ppm): 5.94(s, 1H, H-3), 12.1(s,1H, Ar-OH), 5.35 (d, J = 1.6 Hz, 1H, H-6), 5.64 (d, J = 2 H, 1H ,H-8), 7.09 (d, J = 8.4 Hz, 2H, H-2', 6'), 6.09 (d, J = 8.4 Hz, 2H, H-3', 5').

^{13}C NMR (100 MHz, DMSO-d_6) δ_C (ppm): 94.3 (C-8), 99.2 (C-6), 103.2 (C-3), 104 (C-10), 115.9 (C-3' and 5'), 121.5 (C-1'), 128.5 (C-2' and 6'), 157.7 (C-9), 161.5 (C-5), 161.8 (C-4'), 164.1 (C-2), 182.1 (C-4).

Structure Elucidation of Antidiabetic Active Isolated Compound AAT-3

The diabetic active compound AAT-3, (0.75 %) yield was isolated as yellow crystals from ethyl acetate extract of *B. monnieri,* using a solvent system (PE: EA 1:1). The R_f value is 0.4. It may be a flavonoid compound because it gave off a red colour when treated with Mg/HCl and a brown colour when reacted with 10 % $FeCl_3$. The UV-vis spectrum of AAT-3 showed the flavonoid bands II and I in methanol at 254 nm and 351 nm. This absorption band may be a flavone (bands II 210-280 and band I 310-350). The addition of 2M NaOH shifted the band at λ_{max} 351 nm to 404 nm, i.e., a 53 nm shift of band I, suggesting the presence of an OH group at position 4′. On the other hand, the addition of NaOAc shifted the band at λ_{max} 254 nm to 267 nm, i.e., 13 nm shifted from band II, suggesting the presence of a hydroxy group at position 7. The further addition of H_3BO_3 caused a +23 nm shift of band I, relative to the spectrum of AAT-3 in MeOH solution, suggesting the presence of the *o-di*hydroxy group on the B ring. The presence of

$AlCl_3$ showed a bathochromic in the band I of 55 nm (351 nm to 406 nm) which exhibited *o-di*-OH on the B ring (3'-OH and 4'-OH) adjacent to the C=O group. The presence of an OH group in position 5 was exhibited (Figure 9). After the addition of HCl, the UV-vis spectral properties in various shift reagents of AAT-3 were found to be identical to those of 5, 7, 3' and 4' tetrahydroxy flavone (Rahate and Rajasekaran, 2018).

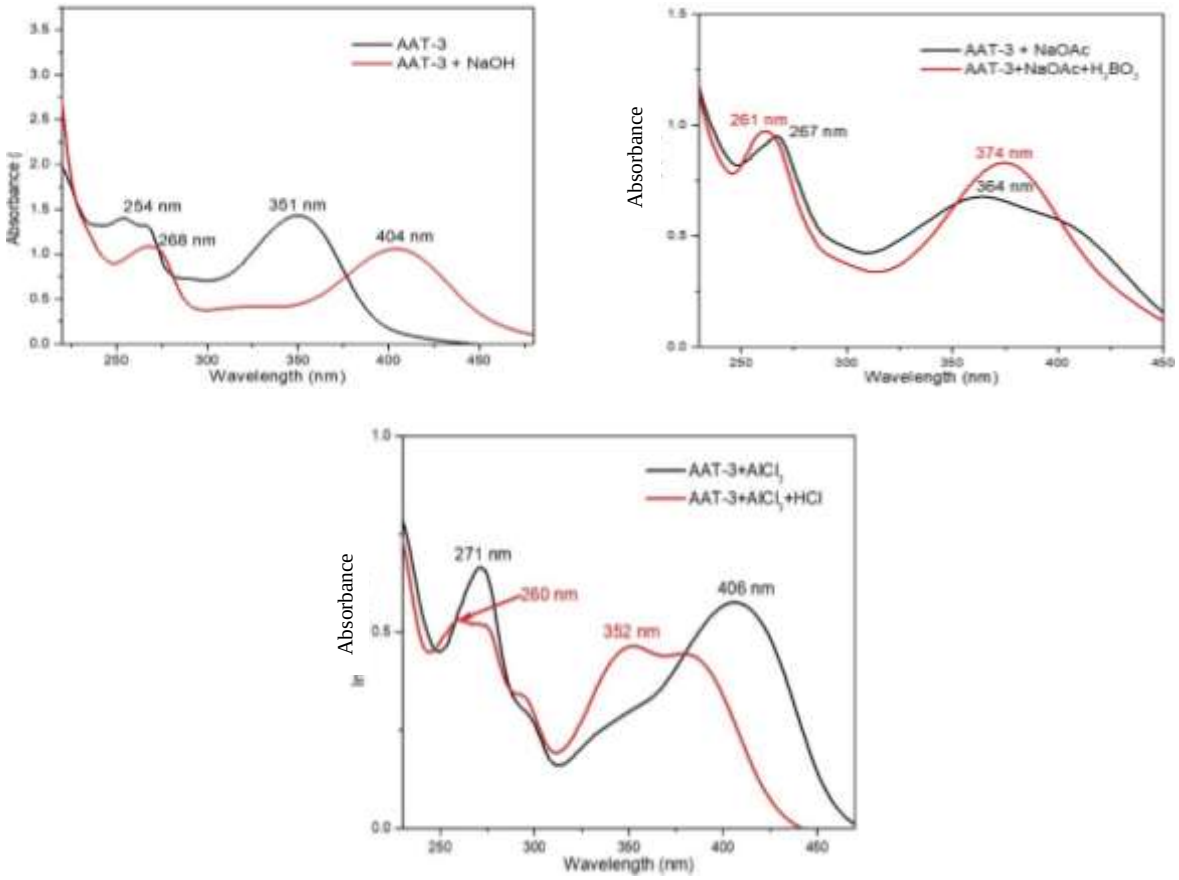

Figure 9. UV spectra of an isolated compound Luteolin (AAT-3) by using shift reagents

In the FT IR spectrum of compound AAT-3, the absorption bands that occurred at 3295 cm^{-1} and 3070 cm^{-1} were indicated due to the O-H stretching band of the phenolic group and the C-H stretching of the aromatic ring. At 1649 cm^{-1}, the C=O stretching of an unsaturated carbonyl group appeared. The bands at 1604 cm^{-1}, 1555 cm^{-1}, and 1495 cm^{-1} were assigned for the C=C stretching of an aromatic ring. The absorption band at 1364 cm^{-1} was due to the O-H bending of the phenolic group, and the absorption bands at 1254 cm^{-1} and 1117 cm^{-1} appeared due to the stretching of the cyclic C-O-C group. The absorption band at 1162 cm^{-1} was assigned as the C-O stretching of the phenolic group. The band at 861 cm^{-1} =C-H out of plane bending vibration of the aromatic system (Figure 10).

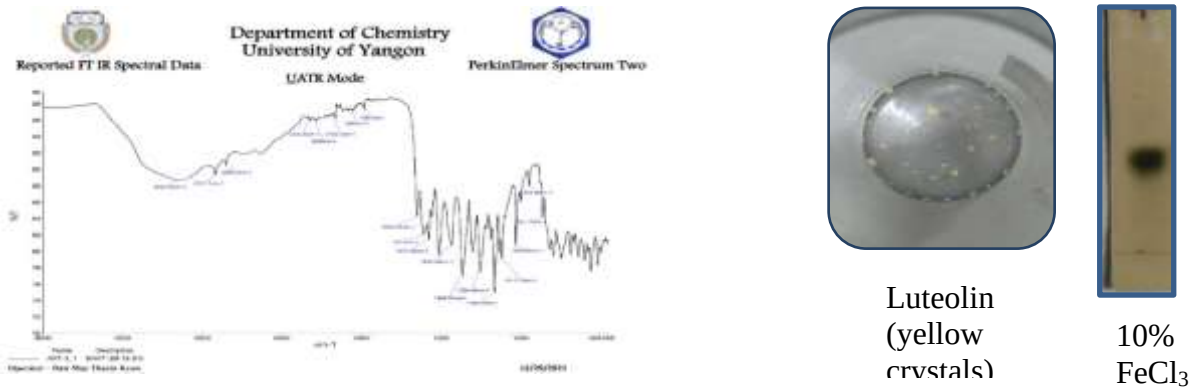

Figure 10. FT IR spectrum of an isolated compound Luteolin (AAT-3)

The ^{1}H NMR spectrum (400 MHz, DMSO-d_6) of the isolated compound AAT-3 showed ten proton signals (Figure 11). A doublet of the doublet with ortho and meta coupling constant (J = 2.4, 8.0 Hz) appeared at δ 7.37 ppm, representing a proton of 6'. A doublet at δ 7.34 ppm (J = 2.4 Hz) was a characteristic of the H-2' proton. In addition, the H-5' proton was observed as a doublet (J = 8.8 Hz) at δ 6.84 ppm. A singlet at δ 6.61ppm was attributed to a proton of H-3. Two singlets at 6.38 and 6.13 ppm corresponded to protons on H-8 and H-6.

The ^{13}C NMR spectrum indicated the presence of 15 signals, which included one carbonyl group, eight quaternary carbon signals, and six methine carbon signals. The ^{13}C NMR spectrum is shown in Figure 11. The carbon signals were observed for six methine signals at δc 145.73 (C-3'), 118.99 (C-6'), 113.36 (C-2'), 102.87 (C-3), 98.82 (C-6) and 93.83 (C-8), eight quaternary carbon signals at δc 164.12 (C-7), 163.88 (C-2), 161.47 (C-5), 157.27 (C-9), 121.49 (C-1'), 116 (C-5'), 103.69 (C-10). One carbonyl signal was also observed at 182.66 (C-4). From the basis of the observed melting point, some physicochemical tests, and all spectral data compared with the reported data of luteolin (Puspalata *et al.*, 2019), the isolated compound AAT-3 was identified as luteolin ($C_{15}H_{15}O_6$).

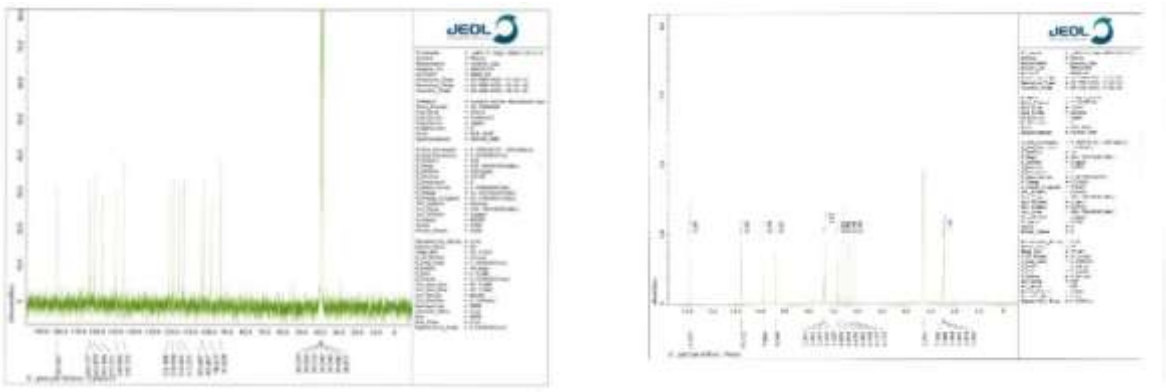

Figure 11. ^{1}H NMR (DMSO-d_6, 400 MHz) and ^{13}C NMR (DMSO-d_6, 100 MHz) spectra of AAT-3

Compound **AAT-3** (Luteolin): A yellow crystal crystallized from PE:EtOAc, mp: 325℃.; FTIR (ν cm^{-1}): 3295(ν_{O-H}), 1649($\nu_{C=O}$), 1611,1577, 1432($\nu_{C=C}$), 1254, 1117 (ν_{C-O-C}), 861(δop (C-), UV_{max} (MeOH) nm: 254, 351; NaOAc nm: 267,364; NaOAc+ H_3BO_3 nm: 261, 374; $AlCl_3$ nm: 271, 406 ; $AlCl_3$ + HCl nm: 260, 352; NaOH nm: 268, 404.^{1}H NMR (400 MHz, DMSO-d_6) δH (ppm): 6.61(s,1H, H-3), 12.92, 10.77, 9.87, 9.349,(s,1H, 5, 7,4', 3'-OH), 7.367 (dd, J =2.4, 8 Hz, 1H, H- 6'), 7.335 (d, J = 2.4 Hz,1 H, H-2'), 6.836 (d, J = 8.8 Hz, 1H, H-5'), 6.382 (d, J = 1.6 Hz,1H, H-8), 6.127 (d, J =1.6 Hz, 1H, H-6) ^{13}C NMR (100 MHz, DMSO-d_6) δ_C (ppm): 93.8

(C-8), 98.8 (C-6),102.88 (C-3),103.69 (C-10) 145.73 (C-3') 121.49 (C-1') 116.01 (C-5'), 118.99(C-'), 113.36 (C-2'), 157.27 (C-9), 161.47 (C-5), 149.68 (C-4'), 164.12 (C-7), 163.88 (C-2), 181.C-4).

The structures of two isolated compounds AAT-2 as apigenin and AAT-3 as luteolin are shown in Figure 12.

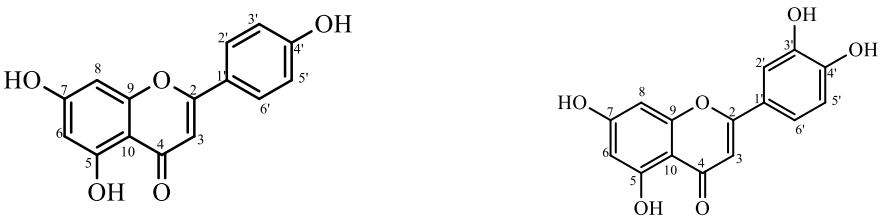

Figure 12. Structures of isolated compounds: AAT-2 (Apigenin) and AAT-3 (Luteolin)

Conclusion

The present study deals with the isolation and identification of apigenin and luteolin from aerial parts of *B, monnieri* and screening for *in vitro* antidiabetic activity. The extraction of phenolic compounds from aerial parts of *B, monnieri* was done by using 70 % ethanol, and the resulting extract was divided into pet ether, ethyl acetate, and water-soluble portions. Apigenin and luteolin were isolated from the ethyl acetate portion by column chromatography. Its structure was identified by modern spectroscopic methods. The ethanol and watery extracts possessed antidiabetic activity due to their α-amylase inhibitory effects (IC_{50}= 54.09 μg/mL, 78.14 μg/mL) and α-glucosidase inhibitory effects (IC_{50} = 62 μg/mL, 91.66 μg/mL) comparable with the standard drug metformin (IC_{50} = 45.31 μg/mL, 50.79 μg/mL). On the other hand, the isolated compounds apigenin and luteolin possessed antidiabetic activity due to their α-amylase inhibitory effects (IC_{50}= 1.049 μg/mL, 0.75 μg/mL) and α-glucosidase inhibitory effects (IC_{50} = 0.558 μg/mL, 0.507 μg/mL) comparable with the standard drug metformin (IC_{50} = 0.497 μg/mL, 0.44 μg/mL). The higher percent enzyme inhibition with the lowest IC_{50} value, the percent inhibition of ethanol extract and luteolin was nearly the same as the percent inhibition of standard metformin.

Acknowledgements

The authors would like to express their profound gratitude to the Department of Higher Education (Lower Myanmar), Ministry of Education, Yangon, Myanmar, for giving them the opportunity to do this research and the Myanmar Academy of Arts and Science for allowing them to present this paper.

References

Ei Shoubaky. G.A., M. Mohamed, H. M. ADaim, H. M. Mohamed, and E. A. Salem. (2016).” Isolation and Identification of a Flavone Apigenin from Marine Red Alga Acanthophora spicifera with Antinociceptive and Anti-Inflammatory Activities”. *Journal of Experimental Neuroscience,* vol.10, pp. 21-29

Ghosh, T., T. K. Maity and J. Singh. (2011). “Antihyperglycemic Activity of Bacosine, A Triterpene from *Bacopa monnieri*, in Alloxan-induced Diabetic Rats”. *Planta Med*., vol.77, pp. 804-808

Kajaria, D., S. Tiwari, J. Tripathi, Tripathi, and Y. Ranjana. (2013) “*In-vitro* α Amylase and Glycosidase Inhibitory Effect of Ethanolic Extract of Antiasthmatic Drug-Shirishadi”. *J. Adv. Pharm. Technol. Res*., vol.4, pp. 206–209

Khadayat, K., P. M Bishnu, G. Hira Gautam, G. Sajani and P. Niranjan. (2020). “Evaluation of the α-Amylase Inhibitory Activity of Nepalese Medicinal Plants Used in the Treatment of Diabetes Mellitus.” *Clinical Phytoscience*, vol.6(34), pp. 1-8

Kim, J., T. Hyun, and M. Kim. (2011).” The Inhibitory Effects of Ethanol Extract from Sorghum, Foxtail Millet and Proso Millet on Glucosidase and α-Amylase activities.” Food α- α Chemistry, vol. 124, pp. 1647-51

Lal, S and B. Baraik. (2019).” Phytochemical and Pharmacological Profile of *Bacopa monnieri* an Ethnomedical Plant”. *JPSR,* vol.10(3), pp. 1001-1013

Mogale, A. M., L. S. Lebelo, N. Thovhogi, A. N. de Freitas, and L. J. Shai. (2011) “*α*-Amylase and *α*-Glucosidase Inhibitory Effects of *Scleroderma Birrea* [(A. Rich.) Hochst.] Subspecies *caffra* (Sond) Kokwaro (Anacardiaceae) Stem-bark Extracts,” *African Journal of Biotechnology*, vol. 10(66), pp. 15033–15039

Ogunwande, A., T. Matsui, T. Fujise, and K. Matsumoto. (2007) “*α*-Glucosidase Inhibitory Profile of Nigerian Medicinal Plants in Immobilized Assay System,” *Food Science and Technology Research*, vol.13(2), pp. 169–178

Oyedemi,S.O., B.O. Oyedemi, Ijeh,I.I.,Ohanayarem,P.E.,Coopoosamy,R.M.,and Aiyegoro,O.A.(2017). “Alpha-Amylase Inhibition and Antioxidative Capacity of Some Antidiabetic Plants Used by the Traditional Healers in Southeastern Nigeria”. *The Scientific World Journal*, vol.10, pp. 1-11

Puspalata, B., P. Parajuli, P. P. Ramesh, and K. S. Jae. (2019). “Microbial Biosynthesis of Antibacterial Chrysoeriol in Recombinant *Escherichia coli* and Bioactivity Assessment.” *Catalysts,* vol.9, pp.1-15

Rahate, K. P., and A. Rajasekaran. (2018).” Isolation and Identification of Flavone Aglycones in Roots of Desmostachya Bipinnata Stapf*”. Indian J Pharm Sci*, vol.80(3), pp. 551-556

Williams, G. (2013). “Possible Effect of Diatary Polyphenol on Sugar Absorption and Digestion”. *Molecular Nutr Food Res*, vol. 57, pp. 48-57